North polar deposits of Mars: Extreme purity of the water ice

Cyril Grima, Wlodek Kofman, Jeremie Mouginot, Roger Phillips, Alain Hérique, Daniela Biccari, Roberto Seu, Marco Cutigni

North polar deposits of Mars: Extreme purity of the water ice

Cyril Grima,[1] Wlodek Kofman,[1] Jérémie Mouginot,[1] Roger J. Phillips,[2] Alain Hérique,[1] Daniela Biccari,[3] Roberto Seu,[3] and Marco Cutigni[3]

Received 13 October 2008; revised 21 December 2008; accepted 31 December 2008; published 12 February 2009.

[1] The polar layered deposits are the largest reservoir of water on the surface of Mars. The physical properties of the ice and their spatial distribution are largely unknown. 140,000 data points from the sounding radar SHARAD on the Mars Reconnaissance Orbiter were analyzed over the Gemina Lingula region, one-fourth of the north polar layered deposits area. Maps of the dielectric properties of the bulk ice were drawn up. There is no basal melting signature. A drop of the dielectric constant in north-west of Gemina Lingula could be explained by an abrupt 250-meter uplift of the base. The bulk ice of the studied region has an average dielectric constant of 3.10 (σ = 0.12) and a loss tangent <0.0026 (σ = 0.0005). Analytic interpretations shown the volume of ice is pure at ≥95%. The impurities have a radial distribution, with higher concentrations at margins. **Citation:** Grima, C., W. Kofman, J. Mouginot, R. J. Phillips, A. Hérique, D. Biccari, R. Seu, and M. Cutigni (2009), North polar deposits of Mars: Extreme purity of the water ice, *Geophys. Res. Lett.*, *36*, L03203, doi:10.1029/2008GL036326.

1. Introduction

[2] The knowledge of the physical properties of the Martian polar deposits is one of the main unresolved questions in Martian polar science [*Clifford et al.*, 2002; *Fishbaugh et al.*, 2008]. In particular, an accurate estimation of the dielectric characteristics is important since it is interrelated to the impurities contamination of the ice and consequently to its rheology [*Durham et al.*, 1992; *Watters et al.*, 2007; *Heggy et al.*, 2007] whereas the spatial distribution of the impurities is linked to the interaction of the ice deposits with the Martian climate. Moreover, it would be a significant contribution for comparative planetology with terrestrial caps since the Martian ice has the same crystalline structure as on Earth but accumulated under an extreme planetary environment (mean surface temperature and pressure of 155 K and 0.008 bar, respectively).

[3] The north polar plateau (Planum Boreum) lies on the widely flat Vastitas Borealis Formation (VBF) recording geological terrains over 3 billions of years. Planum Boreum covers an area of ∼1,000,000 km^2 from 80° of latitude onwards, and is incised by the Chasma Boreale valley over more than 300 km. It includes several geological units. The northern polar layered deposits (NPLD) are made of finely horizontal layers accumulated regularly through its history, with various ice-dust fractions [*Cutts and Lewis*, 1982; *Thomas et al.*, 1992]. Because of the high albedo of the layers, they are thought to be almost pure, but the ice-dust ratio is not precisely known. Although the age of the NPLD unit is unknown, the surface has been dated by cratering records to be <5 Ma, but likely resurfacing-processes would increase this age [*Herkenhoff and Plaut*, 2000; *Tanaka*, 2005]. Between the VBF and the NPLD is located the coarse and dark basal unit (BU) – recently interpreted as the Rupes Tenuis unit with pockets of the Planum Boreum cavi unit [*Tanaka et al.*, 2008] - newly discovered and whose origin is still discussed [*Malin and Edgett*, 2001; *Fishbaugh and Head*, 2005]. The BU has exposures in the surrounding region of Olympia Planitia and across Chasma Boreale [*Phillips et al.*, 2008]. It has been shown that the BU does not extend outward beyond this latter valley, in the Gemina Lingula (GL) region [*Byrne and Murray*, 2002; *Fishbaugh and Head*, 2005]. Thus GL is the only part of the NPLD lying directly on the VBF. GL represents one-fourth of the NPLD area.

2. Data and Method

[4] The interior of the NPLD were deeply probed by The SHAllow RADar (SHARAD) sounder on board the NASA's Mars Reconnaissance Orbiter spacecraft [*Seu et al.*, 2004; *Phillips et al.*, 2008]. SHARAD works at a frequency of 20 MHz. Its penetration depth (i.e., attenuation of the signal) depends of the dielectric properties of the sounded material; typically more than 1 km in water ice. The SHARAD radar signal detects the bottom of the NPLD as a diffused echo (Figure 1), but is attenuated before reaching deeper interfaces at the base of the BU. Basically, in radar science, if the thickness of a deposit is known, its dielectric constant (ε) can be inferred from the time delay between the surface echo and the bottom echo [*Nouvel et al.*, 2006; *Watters et al.*, 2007]:

$$\varepsilon = \left(\frac{tc}{2h}\right)^2 \quad (1)$$

where t is the time delay, c is the speed of light in vacuum, and h is the thickness of the deposit. That is, where the thickness of the NPLD is obtained, its ε can be computed. The VBF has a flat topography with wide wavelengths (∼thousands of kilometers), and is not deflected more than 100 m by Planum Boreum load [*Phillips et al.*, 2008]. We interpolated the VBF topography by a polynomial method under Planum Boreum to have an estimation of the NPLD thickness in the GL region where the ice deposit is in contact with the VBF (Figure 2). This was done by using the MOLA digital elevation model [*Smith et al.*, 2001] with 256 pixels/° and 1 m of vertical resolution. A polynomial of degree 9 was used, for which the mean deviation between the VBF and the interpolated surface damps to ∼35 m

[1]Laboratoire de Planétologie de Grenoble, UJF, CNRS, Grenoble, France.
[2]Southwest Research Institute, Boulder, Colorado, USA.
[3]Dipartimento InfoCom, Università di Roma "La Sapienza", Rome, Italy.

0094-8276/09/2008GL036326

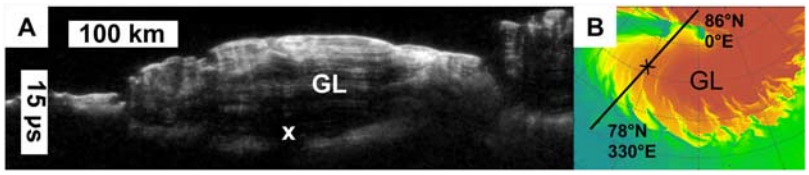

Figure 1. (a) Part of the SHARAD radargram 581302 over GL, with a time y-axis. The bright echo at the top is the surface, while the last diffuse echo is the bedrock. Internal reflections come from the NPLD layering. The cross marks an area of 30 km of spatial extent where basal reflections are absent from all orbits; either due to a bright scattering of the surface or a buried crater with a low floor. (b) Context elevation map of the radargram.

(2.5% of the average GL thickness). For Planum Boreum (i.e., NPLD + BU), we obtained a maximum thickness of 2680 m, and a volume of 1.14×10^6 km^3 between the surface and the interpolated bedrock, similar to that inferred by *Smith et al.* [2001]. Obviously, independently from potential local anomalies, the closer one is from the center of the interpolated zone, the greater are the deviation between the true bedrock and the reconstructed one. This error is minimal since only the GL region close to the border is considered.

[5] We defined GL as the part of Planum Boreum below 84.5°N and between −50°E and 40°E. In this zone, we collected 140,000 SHARAD data points (pulses) for which the surface and the bedrock echoes are both well identified. To determine the vertical position of the diffused bedrock echo, we selected for each pulse the most powerful pixel within an area limiting the whole echo. We avoided scopuli, which are irregular troughs incised in the margin of the NPLD. It is also simple to obtain the loss tangent (tan δ) of the ice from ε and the attenuation of the signal between the surface echo and the one of the bedrock [e.g., *Ulaby et al.*, 1981; *Chyba et al.*, 1998]:

$$\tan\delta = \frac{\alpha/2h}{0.091\nu\sqrt{\varepsilon}} \tag{2a}$$

$$\tan\delta = \frac{10\log_{10}(P_t/P_b)}{0.091\nu\, t\, c} \tag{2b}$$

with

$$P_t = P_s\left[\left(\frac{\sqrt{\varepsilon}+1}{\sqrt{\varepsilon}-1}\right)^2 - 1\right] \tag{2c}$$

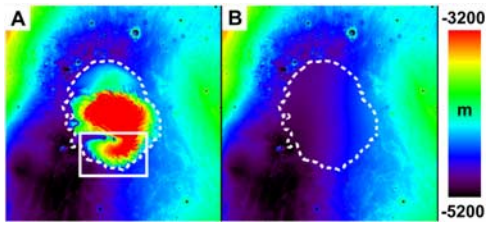

Figure 2. North polar regions of Mars. The dotted white-line demarcates the polar deposits of ice. Each map is a 2650×2650 km^2 square centered on the North Pole. Elevations greater than −3200 m are saturated in red. (a) Digital elevation model (DEM) of the northern polar regions; the white rectangle surrounds GL. (b) Initial DEM of the VBF combined with the bedrock inferred from the interpolation.

Where P_s, P_b and P_t are the power of surface echo, the power of the bedrock echo, and the transmitted power into the deposit, respectively, α is the signal loss into the deposit, and ν is the frequency of SHARAD in MHz.

3. Results

[6] The distribution of both ε and tan δ is approximately Gaussian, though some local heterogeneities contribute to slightly enlarge the flank of the curves (Figure 3). The results give as the most likely values 3.10 for ε and <0.0026 for tan δ of the bulk ice of GL, with a sigma error of 0.12 and 0.0005, respectively (i.e., a 68% confidence interval). One should keep in mind that the value for tan δ is an upper limit as it also includes the contribution of signal losses at each interface reflections. The real loss tangent due exclusively to ice absorption should be strictly lower.

[7] ε is mainly sensitive to the temperature and the volume fraction of impurities in the ice, increasing with both. ε also

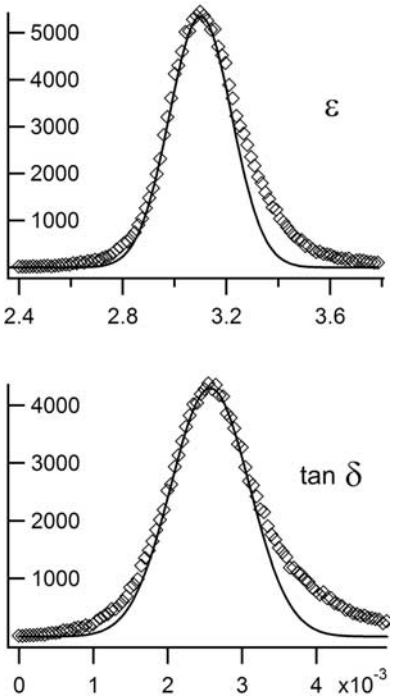

Figure 3. Distribution of the calculated values for (top) ε and (bottom) tan δ of the NPLD. Diamonds are the data integrated over intervals of 0.014 and 0.00005 in width for ε and tan δ, respectively. The y-axis is the total count for each interval. The black line is the Gaussian fitting. The right flank of ε data is larger than the fit due to the contribution of high values before −10°E.

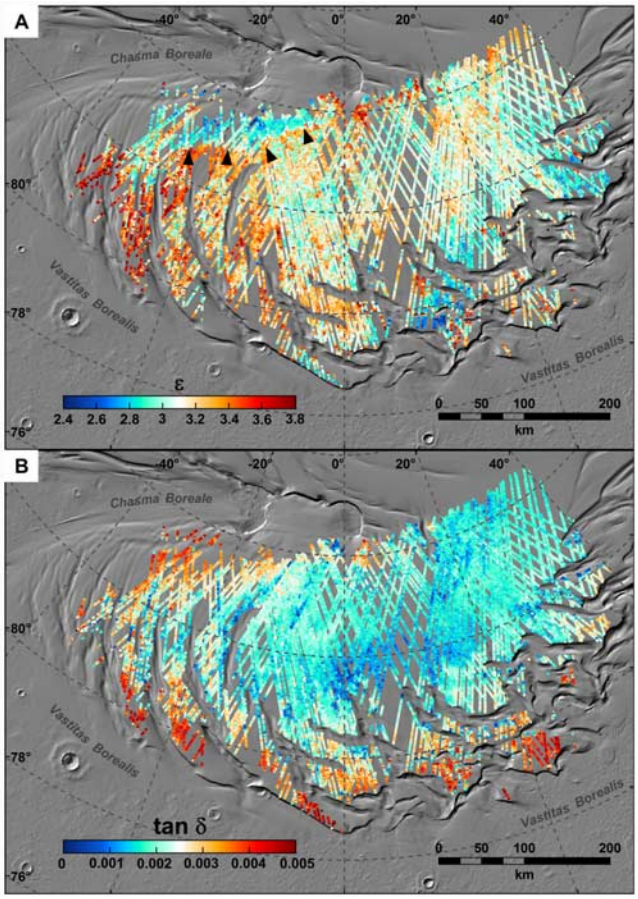

Figure 4. Maps of (a) ε and (b) tan δ of the NPLD over the GL region. Due to the method employed, each point represents the average value for a column of ice down to the base of the NPLD. Black arrows on the top map indicate the $\varepsilon-$drop interpreted as the extent limit of the Rupes Tenuis unit (see text for details).

decreases with the density. However, the influence of the density can be neglected. Indeed, the porosity of the ice declines to zero ~300 m below the surface [*Arthern et al.*, 2000], while the average thickness is 1450 m. The temperature of a column of ice in GL should be in the range of 160 to 220 K, respectively, the mean surface temperature and the expected bedrock temperature [*Larsen and Dahl-Jensen*, 2000]. In the literature, the values of ε for pure water ice under Martian conditions are sparse. To summarize, at radar frequencies similar to that of SHARAD, the ε for pure water ice is in the range of 3.10 to 3.20 for temperatures above 200 K to 273 K [e.g., *Gough*, 1972; *Johari*, 1976; *Petrenko and Whitworth*, 1999], while it falls down to 3.0 below [*Gough*, 1972; *Heggy et al.*, 2007]. Thus the difference between our inferred value of 3.10 and the true one for pure water ice appears to be no more than 0.10. In this range of ε (3.0 to 3.2), the impurity rate corresponding to a 10% variation of ε can be computed by applying the Maxwell-Garnett formula [*Sihvola*, 1999]:

$$\varepsilon_{\text{eff}} = \varepsilon_e + 3f\varepsilon_e \frac{\varepsilon_i - \varepsilon_e}{\varepsilon_i + 2\varepsilon_e - f(\varepsilon_i - \varepsilon_e)} \quad (3)$$

where ε_{eff}, ε_e and ε_i are the dielectric constant of the mixture, the environment, and that of the inclusions, respectively. f is the impurities fraction of the total volume. Admitting the inclusions are basaltic materials with an ε_i in the range of 6 to 8, we found the impurity rate could not exceed 5% in the worst case. This analytic result should be compared with experimental approaches in the future. Ongoing experiences leading by *Heggy et al.* [2007], show that ε = 3.10 could imply an impurity rate up to 10% at Martian conditions.

[8] Tan δ is chiefly sensitive to the impurities fraction, increasing with it. But a significant work aiming to determine precisely tan δ of ice at Martian conditions has yet to be published. However, values between <0.0010 and 0.0050 are commonly used for pure water ice [e.g., *Plaut et al.*, 2007; *Watters et al.*, 2007]. Our value of <0.0026 is in the lower part of this range and confirms the ice should be extremely pure. The layering of the NPLD is continuous and horizontally homogeneous all over its area [*Milkovich and Head*, 2005; *Phillips et al.*, 2008]. Therefore, the global dielectric properties found for GL could be easily generalized to the entire NPLD.

[9] The spatial distribution of ε cannot be simply interpreted in terms of properties of the ice (Figure 4a). Indeed, there is also a contribution of the unknown slight difference between the true thickness of the NPLD and that inferred from our interpolated bedrock. However, there is a region in north-west of Gemina Lingula where ε drops suddenly, on a distance less than 10 km, from an average value of ~3.30 to ~2.95 (red to blue on the map). In this area the mean thickness of the ice is 1300 m. A loss of density is hard to suggest for the reasons explained before, while a sudden elevation of the average temperature of the ice is physically difficult to explain. The other possibility is a rising of the true base of the NPLD above our interpolated bedrock. The corresponding average uplift would be ~250 m. From stratigraphic studies *Tanaka et al.* [2008] suggested that the Rupes Tenuis unit (main element of the BU) - which is partly exposed in Chasma Boreale over Hyperborea Lingula - could continue below the north-west part of GL. Our observation strongly supports this hypothesis of an extent of the Rupes Tenuis unit as far as 80 km under GL.

[10] Although we cannot describe quantitatively a value of tan δ, we can conclude on its relative spatial fluctuations in terms of impurities variations, since it is weakly linked to the inferred thickness of the ice. Its mapping (Figure 4b) clearly shows that tan δ is constantly higher at margins than at the center of GL. Due to the stronger dependence of tan δ with the impurities rate, we conclude the concentration of impurities in the ice is steadily higher at margins.

[11] It has been proposed that basal ice of both polar layered deposits could melt under ice thicknesses more than 4 to 6 km, or at lower depth in a case of geothermal anomalies [*Clifford*, 1987]. There is a high contrast between the dielectric constant of water ice and liquid water (20 to 30 times more for the latter). If basal melting is occurring in GL (1800 m of maximum thickness), its signature should be clear on the tan δ map since it has been calculated from the power ratio between the surface and the bedrock echo. There is no such signature; we conclude there is no geothermal anomaly leading to basal melting in the GL region at present.

[12] **Acknowledgments.** The Shallow Radar (SHARAD) was provided by the Italian Space Agency, and its operations are led by the InfoCom Department, University of Rome "La Sapienza". Thales Alenia Space Italia is the prime contractor for SHARAD and is in charge of in-flight instrument and of the SHARAD Operations Center. The Mars Reconnaissance Orbiter mission is managed by the Jet Propulsion Laboratory, California Institute of Technology, for the NASA Science Mission Directorate, Washington, DC. Lockheed Martin Space Systems, Denver, is the prime contractor of the orbiter. The authors are grateful to the European space agency (ESA) and the French space agency (CNES) for supporting this work. We thank Jérémie Lassue for his careful review.

References

Arthern, R. J., D. P. Winebrenner, and E. D. Waddington (2000), Densification of water ice deposits on the residual north polar cap of Mars, *Icarus*, *144*, 367–381.

Byrne, S., and B. C. Murray (2002), North polar stratigraphy ad the paleo-erg of Mars, *J. Geophys. Res.*, *107*(E6), 5044, doi:10.1029/2001JE001615.

Chyba, C. F., S. J. Ostro, and B. C. Edwards (1998), Radar detectability of a subsurface ocean on Europa, *Icarus*, *134*, 292–302.

Clifford, S. M. (1987), Polar basal melting on Mars, *J. Geophys. Res.*, *92*, 9135–9152.

Clifford, S. M., et al. (2002), The state and future of Mars polar exploration, *Icarus*, *144*, 210–242.

Cutts, J. A., and B. H. Lewis (1982), Models of climatic cycles recorded in Martian polar layered deposits, *Icarus*, *50*, 216–244.

Durham, W. B., S. H. Kirby, and L. A. Stern (1992), Effects of dispersed particulates on the rheology of water ice at planetary conditions, *J. Geophys. Res.*, *97*, 20,883–20,897.

Fishbaugh, K. E., and J. W. Head (2005), Origin and characteristics of the Mars north polar basal unit and implications for polar geologic history, *Icarus*, *174*, 444–474.

Fishbaugh, K. E., et al. (2008), Introduction to the 4th Mars polar science conference special issue: Five top questions in Mars polar science, *Icarus*, *196*, 305–317.

Gough, S. R. (1972), A low temperature dielectric cell and the permittivity of hexagonal ice to 2 K, *Can. J. Chem.*, *50*, 3046–3051.

Heggy, E., et al. (2007), Geoelectrical model of the Martian north polar layered deposits, *Lunar Planet. Sci.*, *XXXIX*, Abstract 2471.

Herkenhoff, K. E., and J. J. Plaut (2000), Surface ages and resurfacing rates of the polar layered deposits on Mars, *Icarus*, *144*, 243–253.

Johari, G. P. (1976), The dielectric properties of H_2O and D_2O ice Ih at MHz frequencies, *J. Chem. Phys.*, *64*, 3998–4004.

Larsen, J., and D. Dahl-Jensen (2000), Interior temperatures of the northern polar cap of Mars, *Icarus*, *144*, 456–462.

Malin, M. C., and K. S. Edgett (2001), Mars Global Surveyor Mars Orbiter Camera: Interplanetary cruise through primary mission, *J. Geophys. Res.*, *106*, 23,429–23,570.

Milkovich, S. M., and J. W. Head (2005), North polar cap of mars: Polar layered deposit characterization and identification of a fundamental climate signal, *J. Geophys. Res.*, *110*, E01005, doi:10.1029/2004JE002349.

Nouvel, J.-F., J.-E. Martelat, A. Herique, and W. Kofman (2006), Top layers characterization of the Martian surface: Permitivity estimation based on geomorphology analysis, *Planet. Space Sci.*, *54*, 337–344.

Petrenko, V. F., and R. W. Whitworth (Eds.) (1999), *Physics of Ice*, Oxford Univ. Press, New York.

Phillips, R. J., et al. (2008), Mars north polar deposits: Stratigraphy, age, and geodynamical response, *Science*, *320*, 1182–1185.

Plaut, J. J., et al. (2007), Subsurface radar sounding of the south polar layered deposits of Mars, *Science*, *316*, 92–96.

Seu, R., et al. (2004), SHARAD: The MRO 2005 shallow radar, *Planet. Space. Sci.*, *52*, 157–166.

Sihvola, A. (Ed.) (1999), *Electromagnetic Mixing Formulas and Applications*, Inst. of Electr. Eng., London.

Smith, D. E., et al. (2001), Mars Orbiter Laser Altimeter: Experiment summary after the first year of global mapping of Mars, *J. Geophys. Res.*, *106*, 23,689–23,722.

Tanaka, K. L. (2005), Geology and insolation-driven climatic history of Amazonian north polar materials on Mars, *Nature*, *437*, 991–994.

Tanaka, K. L., et al. (2008), North polar region of Mars: Advances in stratigraphy, structure, and erosional modification, *Icarus*, *196*, 318–358.

Thomas, P. C., S. W. Squyres, K. E. Herkenhoff, A. D. Howard, and B. C. Murray (1992), Polar deposits of Mars, in *Mars*, edited by H. H. Kieffer et al., pp. 767–795, Univ. of Arizona Press, Tucson.

Ulaby, F. T., R. K. Moore, and A. K. Fung (Eds.) (1981), *Microwave Remote Sensing*, vol. 1, Artech House, Norwood, Mass.

Watters, T. R., et al. (2007), Radar sounding of the Medusae Fossae formation Mars: Equatorial ice or dry, low-density deposits?, *Science*, *318*, 1125–1128.

D. Biccari, M. Cutigni, and R. Seu, Dipartimento InfoCom, Università di Roma "La Sapienza", I-00184 Rome, Italy.

C. Grima, A. Hérique, W. Kofman, and J. Mouginot, Laboratoire de Planétologie de Grenoble, UJF, CNRS, F-38041 Grenoble CEDEX, France. (cyril.grima@obs.ujf-grenoble.fr)

R. J. Phillips, Southwest Research Institute, Boulder, CO 80302, USA.